sults indicate that the singularity of VSG expression and the semiordered appearance of VSGs in *T. brucei* infections (*10*, *27*) are probably determined at the level of ES transcription rather than imposed by intrinsic constraints on VSG compatibility. This interpretation is consistent with the previously demonstrated instability of cells expressing two VSGs from different ESs (*9*). Perhaps expressing one VSG at a time has evolved as simply the most economical strategy of immune evasion, but some other product of an ES is responsible for imposing singularity, for reasons that remain to be identified.

REFERENCES AND NOTES:

1. G. A. M. Cross, *Annu. Rev. Immunol.* **8**, 83 (1990); L. Vanhamme and E. Pays, *Microbiol. Rev.* **59**, 223 (1995); G. A. M. Cross, *Bioessays* **18**, 283 (1996).
2. L. H. T. Van der Ploeg *et al.*, *Nucleic Acids Res.* **10**, 5905 (1982).
3. D. F. Cully, H. S. Ip, G. A. M. Cross, *Cell* **42**, 173 (1985); M. Navarro and G. A. M. Cross, *Mol. Cell. Biol.* **16**, in press.
4. J. M. Kooter *et al.*, *Cell* **51**, 261 (1987); M. Crozatier, L. H. T. Van der Ploeg, P. J. Johnson, J. Gommers-Ampt, P. Borst, *Mol. Biochem. Parasitol.* **42**, 1 (1990); S. Lips, P. Revelard, E. Pays, *ibid.* **62**, 135 (1993).
5. A. Bernards *et al.*, *Cell* **36**, 163 (1984).
6. K. M. Esser and M. J. Schoenbechler, *Science* **229**, 190 (1985).
7. C. M. Alarcon, H. J. Son, T. Hall, J. E. Donelson, *Mol. Cell. Biol.* **14**, 5579 (1994); S. V. Graham, K. R. Matthews, P. G. Shiels, J. D. Barry, *Parasitology* **101**, 361 (1990); S. V. Graham and J. D. Barry, *Mol. Biochem. Parasitol.* **47**, 31 (1991); S. V. Graham, *Parasitol. Today* **11**, 217 (1995).
8. D. Salmon *et al.*, *Cell* **78**, 75 (1994); M. J. L. Ligtenberg *et al.*, *EMBO J.* **13**, 2565 (1994); D. Steverding, Y.-D. Stierhof, H. Fuchs, R. Tauber, P. Overath, *J. Cell Biol.* **131**, 1173 (1995).
9. T. Baltz *et al.*, *Nature* **319**, 602 (1986).
10. Z. Agur, D. Abiri, L. H. T. Van der Ploeg, *Proc. Natl. Acad. Sci. U.S.A.* **86**, 9626 (1989).
11. Z. Agur, *Parasitol. Today* **8**, 128 (1992); *ibid.* **11**, 24 (1995); H. T. M. Timmers, T. De Lange, J. M. Kooter, P. Borst, *J. Mol. Biol.* **184**, 81 (1987); D. Barry and C. M. J. Turner, *Parasitol. Today* **8**, 128 (1992); P. Borst and G. Rudenko, *Science* **264**, 1872 (1994); B. G. Williams, D. J. Rogers, C. M. W. Turner, J. D. Barry, Trypanosomiasis and Leishmaniasis Seminar, Glasgow, UK, September 1995.
12. G. A. M. Cross, *Parasitology* **71**, 393 (1975).
13. M. Carrington *et al.*, *J. Mol. Biol.* **221**, 823 (1991).
14. J. G. Johnson and G. A. M. Cross, *J. Protozool.* **24**, 587 (1977); D. Horn and G. A. M. Cross, *Cell* **83**, 555 (1995).
15. G. Allen, L. P. Dicken, G. A. M. Cross, *J. Mol. Biol.* **157**, 527 (1982); G. Allen and L. P. Gurnett, *Biochem. J.* **209**, 481 (1983); J. C. Boothroyd, C. A. Paynter, S. L. Coleman, G. A. M. Cross, *J. Mol. Biol.* **157**, 547 (1982).
16. D. Freymann *et al.*, *J. Mol. Biol.* **216**, 141 (1990).
17. M. L. Blum *et al.*, *Nature* **362**, 603 (1993).
18. M. A. J. Ferguson and A. F. Williams, *Annu. Rev. Biochem.* **57**, 285 (1988); G. A. M. Cross, *Annu. Rev. Cell Biol.* **6**, 1 (1990).
19. R. Bulow and P. Overath, *J. Biol. Chem.* **261**, 11918 (1986); M. Carrington, R. Bulow, H. Reinke, P. Overath, *Mol. Biochem. Parasitol.* **33**, 289 (1989); J. A. Fox, M. Duszenko, M. A. J. Ferguson, M. G. Low, G. A. M. Cross, *J. Biol. Chem.* **261**, 15767 (1986).
20. Partially purified preparations of solubilized VSG were obtained by endogenous GPI-PLC digestion essentially as described [G. A. M. Cross, *J. Cell. Biochem.* **24**, 79 (1984)] but on a microscale. Briefly, 1×10^8 trypanosomes were pelleted and washed two times with trypanosome dilution buffer (*12*), resuspended in deionized water at 0°C, and incubated on ice for 5 min. Cells were centrifuged, resuspended in 100 μl of 10 mM phosphate buffer (pH 8.0), and incubated for 5 min at 37°C. Cells were pelleted again, and one-tenth of the supernatant was used for SDS-PAGE. The 10% polyacrylamide gels were blotted onto nitrocellulose filters, which were reacted with rabbit antibodies raised against individual VSGs, by standard procedures, followed by peroxidase-conjugated goat antibody to rabbit (anti-rabbit) immunoglobulin G (IgG), according to ECL kit specifications (Amersham, UK). The rabbit antibodies to VSGs 121 and 221 had been depleted of cross-reactive antibodies to the GPI anchors by passage over a column of VSG 117. For metabolic labeling, 1×10^8 bloodstream-form *T. brucei* grown in vitro were transferred into 10 ml of methionine-free RPMI (Gibco BRL, Gaithersburg, MD) supplemented with 10% (v/v) dialyzed fetal bovine serum, 10% dialyzed Serum Plus (JRH Biosciences, Lenexa, KS), and incubated with 50 μCi of ^{35}S-labeled methionine-cysteine mixture for 2 hours. VSGs were extracted as described above and samples were immunoprecipitated with cross-reacting determinant–depleted rabbit antibodies to VSG221 coupled to protein A–Sepharose (Pharmacia-LKB).
21. M.-L. Cardoso de Almeida, L. M. Allan, M. J. Turner, *J. Protozool.* **31**, 53 (1984).
22. G. S. Lamont, R. S. Tucker, G. A. M. Cross, *Parasitology* **92**, 355 (1986).
23. C. M. R. Turner and J. D. Barry, *ibid.* **99**, 67 (1989).
24. R. Bulow, C. Nonnengasser, P. Overath, *Mol. Biochem. Parasitol.* **32**, 85 (1989); A. Seyfang, D. Mecke, M. Duszenko, *J. Protozool.* **37**, 546 (1990); M. Duszenko and A. Seyfang, in *Advances in Cell and Molecular Biology of Membranes: Membrane Traffic in Protozoa* (JAI, Greenwich, CT, 1993), vol. 2B, pp. 227–258; B. Ehlers, J. Czichos, P. Overath, *Mol. Cell. Biol.* **7**, 1242 (1987).
25. S. E. Zamze *et al.*, *Eur. J. Biochem.* **187**, 657 (1990); S. E. Zamze, D. A. Ashford, E. W. Wooten, T. W. Rademacher, R. A. Dwek, *J. Biol. Chem.* **266**, 20244 (1991); A. M. Strang, A. K. Allen, A. A. Holder, H. Van Halbeek, *Biochem. Biophys. Res. Commun.* **196**, 1430 (1993).
26. A. W. Cornelissen, P. J. Kooter, J. M. Johnson, L. H. T. Van der Ploeg, P. Borst, *Cell* **41**, 825 (1985).
27. A. R. Gray and A. G. Luckins, in *Biology of the Kinetoplastida*, W. H. R. Lumsden and D. A. Evans, Eds. (Academic Press, London, 1976), vol. 1, pp. 493–542; R. J. Kosinski, *Parasitology* **80**, 343 (1980); E. N. Miller and M. J. Turner, *ibid.* **82**, 63 (1981); P. J. Myler, A. L. Allen, N. Agabian, K. Stuart, *Infect. Immun.* **47**, 684 (1985).
28. A. Y. C. Liu, L. H. T. Van der Ploeg, F. A. M. Rijsewijk, P. Borst, *J. Mol. Biol.* **167**, 57 (1983); J. K. Scholler, R. F. Aline, K. D. Stuart, *Mol. Biochem. Parasitol.* **29**, 89 (1988); R. F. Aline, J. K. Scholler, K. Stuart, *ibid.* **32**, 169 (1989).
29. V. B. Carruthers, L. H. T. van der Ploeg, G. A. M. Cross, *Nucleic Acids Res.* **21**, 2537 (1993).
30. H. Hirumi and K. Hirumi, *J. Parasitol.* **75**, 985 (1989).
31. V. B. Carruthers and G. A. M. Cross, *Proc. Natl. Acad. Sci. U.S.A.* **89**, 8818 (1992).

32. Supported by NIH (grant AI 21531). We thank M. Carrington for supplying the MITat 1.6 clone 121 cDNA and V. B. Carruthers for advice in the early stages of this project and for constructing the initial ES-targeting plasmids from which the vectors used in the present studies were developed. We thank other members of the laboratory for their suggestions and M. Nussenzweig for the use of his PhosphorImager.

22 December 1995; accepted 1 April 1996

Binding of Zinc Finger Protein ZPR1 to the Epidermal Growth Factor Receptor

Zoya Galcheva-Gargova, Konstantin N. Konstantinov, I-Huan Wu, F. George Klier, Tamera Barrett, Roger J. Davis*

ZPR1 is a zinc finger protein that binds to the cytoplasmic tyrosine kinase domain of the epidermal growth factor receptor (EGFR). Deletion analysis demonstrated that this binding interaction is mediated by the zinc fingers of ZPR1 and subdomains X and XI of the EGFR tyrosine kinase. Treatment of mammalian cells with EGF caused decreased binding of ZPR1 to the EGFR and the accumulation of ZPR1 in the nucleus. The effect of EGF to regulate ZPR1 binding is dependent on tyrosine phosphorylation of the EGFR. ZPR1 therefore represents a prototype for a class of molecule that binds to the EGFR and is released from the receptor after activation.

The EGFR is a transmembrane glycoprotein with an extracellular ligand-binding domain and a cytoplasmic tyrosine kinase domain (*1*). EGF treatment causes increased EGFR tyrosine kinase activity. Substrates for the activated receptor tyrosine kinase include the COOH-terminal region of the receptor (*1*). The tyrosine-phosphorylated EGFR binds to modular signaling proteins that contain SRC homology 2 (SH2) or PTB (phosphotyrosine-binding) domains (*1*, *2*). However, before the formation of the receptor signaling complex with SH2-PTB proteins, the EGFR may interact with other proteins (*1*). The identities of the proteins within this complex have not been defined, but these components may include actin and other cytoskeletal proteins (*3*). Proteins bound to the EGFR may also include signaling molecules that are released from the receptor after activation.

The purpose of this study was to identify proteins that bind to the nonactivated

Z. Galcheva-Gargova, I-H. Wu, T. Barrett, R. J. Davis, Program in Molecular Medicine, Department of Biochemistry and Molecular Biology, University of Massachusetts Medical School and Howard Hughes Medical Institute, Worcester, MA 01605, USA.
K. N. Konstantinov and F. G. Klier, Department of Molecular and Experimental Medicine, and Department of Cell Biology, Scripps Research Institute, La Jolla, CA 92037, USA.
*To whom correspondence should be addressed.

EGFR, and we describe here the molecular cloning of the zinc finger protein ZPR1. Recently, zinc finger proteins have been implicated as an important class of receptor-interacting molecules. Examples include a LIM domain protein (enigma) that binds to the insulin receptor (*4*) and ring finger proteins (TRAF, CRAF, and LAP) that bind to the tumor necrosis factor receptor, CD40, and Epstein-Barr virus latent infection membrane protein 1 (*5*). ZPR1 represents a novel class of zinc finger protein that binds to the EGFR.

We used a two-hybrid screen to identify proteins that bind to the COOH-terminal region of the EGFR (*6*). This screen was biased toward the identification of proteins that bind to the EGFR in the absence of tyrosine phosphorylation. Ten positive clones were isolated from a murine fetal cDNA library. Sequence analysis demonstrated that these clones correspond to fragments of five different cDNAs. One of these cDNAs was independently isolated six times and was chosen for further analysis. A full-length murine cDNA clone [2162 base pair (bp)] was obtained by screening an NIH 3T3 cDNA library. The protein encoded by this cDNA was designated ZPR1 (Fig. 1A). Examination of the ZPR1 sequence demonstrated that its NH_2-terminal region was similar to its COOH-terminal region (Fig. 1B). Each of these regions contains a putative zinc finger encoded by amino acids Cys-X_2-Cys-X_{25}-Cys-X_2-Cys (where X_y represents a series of y amino acids). The presence of both zinc fingers was confirmed by the identification of 1.9 ± 0.1 mol of zinc per mole of ZPR1 protein (mean ± SE, n = 3) with inductively coupled plasma emission spectroscopy (*7*). Northern blot analysis demonstrated that the 2.1-kb ZPR1 mRNA was widely expressed in various tissues (Fig. 1C). The largest amounts of ZPR1 were detected in testis tissue. Protein immunoblot analysis with an antibody to a peptide derived from ZPR1 detected a 51-kD protein (Fig. 1D). A large increase in ZPR1 expression was detected after transfection of cells with a ZPR1 expression vector (Fig. 1D).

The isolation of ZPR1 cDNA clones by an interaction trap suggests that ZPR1 binds to the EGFR. We therefore examined the binding of ZPR1 to the EGFR in vitro (Fig. 2A). Bound EGFRs were detected by protein immunoblot analysis with a monoclonal antibody to the EGFR. This analysis demonstrated that the EGFR binds to ZPR1

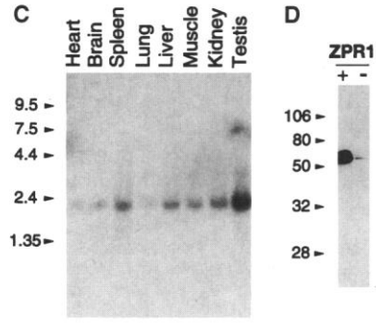

Fig. 1. ZPR1, a zinc finger protein. (**A**) The ZPR1 primary sequence deduced from the nucleotide sequence of the cDNA (*17*). The ZPR1 nucleotide sequence (2162 bp) has been deposited in GenBank with accession number U41287. The Cys residues that form the zinc fingers are indicated with asterisks. (**B**) The NH_2-terminus of ZPR1 is similar to the COOH-terminus. Gaps introduced to optimize the alignment are indicated with a dash. Identical residues are illustrated with a period. (**C**) The expression of ZPR1 in various murine tissues was examined by Northern blot analysis of polyadenylated mRNA (*6*). The position of RNA standards (in kilobases) is indicated on the left. (**D**) The expression of ZPR1 in COS cells was examined by protein immunoblot analysis (*18*). The cells were transfected with an empty expression vector or a ZPR1 expression vector (*10*). The blot was probed with a rabbit polyclonal antibody to a synthetic peptide antigen that corresponds to the ZPR1 COOH-terminus (*18*). The position of protein standards (in kilodaltons) is indicated on the left.

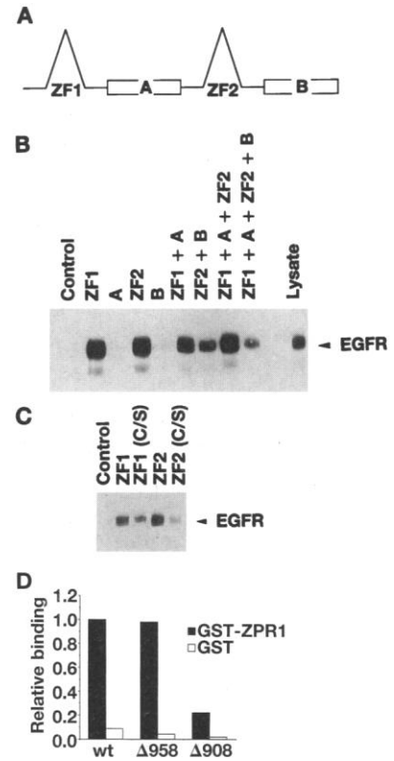

Fig. 2. Binding of ZPR1 to the EGFR tyrosine kinase domain. (**A**) The predicted domain structure of ZPR1 includes two zinc fingers (ZF1 and ZF2) and two regions adjacent to the fingers (A and B). (**B**) GST-ZPR1 was immobilized on glutathione-agarose beads and incubated with cell lysates prepared from A-431 cells (*19*). The beads were extensively washed, and the bound EGFRs were detected by protein immunoblot analysis (*18*). An aliquot of the cell lysate (5%) used for the binding assays was also examined by immunoblot analysis. Control experiments were done with immobilized GST. The functional domains of ZPR1 were examined by deletion analysis (ZF1, residues 1 to 86; A, residues 87 to 255; ZF2, residues 256 to 294; and B, residues 295 to 439). (**C**) Effect of mutation of the ZPR1 zinc fingers (ZF1 and ZF2) on EGFR binding. Cys^{81} and Cys^{84} (ZF1) and Cys^{288} and Cys^{291} (ZF2) were replaced with Ser (C/S) (*8*). (**D**) Deletion analysis of EGFR binding to ZPR1. The wild-type (wt) EGFR and COOH-terminal truncation mutants (Δ958 and Δ908) were translated in vitro with [^{35}S]methionine (*19*). The translated EGFRs were incubated with immobilized GST-ZPR1 (*19*). Control experiments were performed with immobilized GST. Bound EGFRs were detected by SDS-PAGE and PhosphorImager analysis. The relative binding of the EGFRs is presented.

(Fig. 2B). Deletion analysis indicated that the zinc fingers were sufficient for the EGFR binding interaction (*8*). Indeed, a larger amount of EGFR bound to the isolated zinc fingers than to the full-length protein (9). Both zinc fingers bound to the EGFR (Fig. 2B). This binding interaction was reduced (but not eliminated) by mutation of the Cys residues that form the zinc fingers (Fig. 2C). These data demonstrate that ZPR1 binds to the EGFR and that this interaction requires the zinc fingers.

To identify the region of the EGFR that is required for binding to the ZPR1 zinc fingers, we examined the effect of deletions of the COOH-terminal region of the EGFR on the binding interaction. In initial experiments, we examined the effect of proteolytic cleavage of the COOH-terminus of the EGFR with calpain (*10*). We found that both the wild-type and the calpain-cleaved EGFR bound to the ZPR1 zinc fingers (*11*). The major sites of calpain cleavage of the EGFR are Gln^{996} and Asp^{1059} (*12*). The COOH-terminus of the EGFR (residues 996 to 1186) is therefore not required for interaction with ZPR1. In contrast, ZPR1 bound to the COOH-terminal region of the EGFR (residues 908 to 1186) in the yeast two-hybrid analysis. These data suggest that the region of the EGFR required for interaction with ZPR1 corresponds to residues 908 to 996. To test this hypothesis, we prepared [^{35}S]methionine-labeled EGFRs by in vitro translation. Binding of the wild-type EGFR to ZPR1 was detected (Fig. 2D). Truncation of the receptor at residue 958 caused a small decrease in binding to ZPR1. In contrast, truncation at residue 908 caused a marked decrease in EGFR binding to ZPR1. Together, these data demonstrate that a specific region of the EGFR (including residues 908 to 958) is required for binding to ZPR1.

Residues 908 to 958 of the EGFR correspond to subdomains X and XI of the tyrosine kinase domain. This region is highly conserved in members of the EGFR family (HER1, HER2, HER3, and HER4). A related sequence is found in the platelet-derived growth factor (PDGF) receptor, but the sequence differs for other receptor tyrosine kinases. Examination of the conserved tyrosine kinase domain secondary structure indicates that subdomains X and XI include three α helices (G, H, and I) that form a surface at the base of the kinase domain (*13*). This surface may represent the site of interaction of the ZPR1 zinc fingers with the EGFR and is distinct from the tyrosine-phosphorylated COOH-terminal region of the EGFR that binds SH2 and PTB proteins (*1*, *2*).

The conserved secondary structure of the region of the EGFR that is required for ZPR1 binding suggests that other protein kinases may interact with ZPR1. Control experiments demonstrated that ZPR1 did not bind to MAP (mitogen-activated protein) kinase (ERK, JNK, and p38), MAP kinase kinase (MKK1, MKK3, and MKK4), TrkA, the insulin receptor, or the IGF-1 (insulin-like growth factor) receptor (*11*). However, both the PDGF receptor and the EGFR bound to ZPR1 (*11*). Together, these data demonstrate that ZPR1 binds selectively to a subgroup of receptor protein kinases that includes the EGFR.

We next examined the effect of EGF on the binding of the EGFR to ZPR1. Extracts from control cells and EGF-treated cells were incubated with immobilized ZPR1. Treatment with EGF caused decreased binding of the EGFR to ZPR1 (Fig. 3A). The effect of EGF to decrease binding was observed in experiments using either ZPR1 or the ZPR1 zinc fingers (Fig. 3A), was rapid (5 min), and occurred before EGFR down-regulation (Fig. 3B). In contrast to the effect of EGF, treatment of cells with phorbol myristate acetate caused no change in EGFR binding to ZPR1 (*11*). To confirm that EGF regulates the interaction between the EGFR and ZPR1 in vivo, we performed co-immunoprecipitation analysis. ZPR1 was isolated from cell extracts by immunoprecipitation with an antibody to ZPR1. Protein immunoblot analysis demonstrated the presence of EGFRs in the ZPR1 immunoprecipitates (Fig. 3C). In contrast, EGFRs were not detected in immunoprecipitates of ZPR1 prepared from EGF-treated cells (Fig. 3C). Together, these data indicate that ZPR1 interacts with the EGFR in vivo and that the formation of this complex is negatively regulated by EGF. The mechanism of negative regulation may be mediated by the presence of ZPR1 binding proteins in extracts of EGF-treated cells or by decreased affinity of the ZPR1-EGFR interaction.

Treatment of cells with EGF causes increased binding of the receptor to SH2 and PTB signaling proteins (*1*, *2*) and decreased binding of the EGFR to ZPR1 (Fig. 3). This difference was confirmed by direct comparison of the interaction of the EGFR with ZPR1 and the NH_2-terminal SH2 domain of phospholipase C–γ (PLC-γ) (Fig. 4). The interaction of the EGFR with SH2 and PTB proteins requires tyrosine phosphorylation of the receptor (*1*, *2*).

Cell extracts prepared without the tyrosine phosphatase inhibitor orthovanadate contained EGFRs that were not tyrosine phosphorylated and did not bind to the NH_2-terminal SH2 domain of PLC-γ (Fig. 4). Similarly, the tyrosine phosphatase inhibitor orthovanadate was required for the regulation of ZPR1 binding to the EGFR

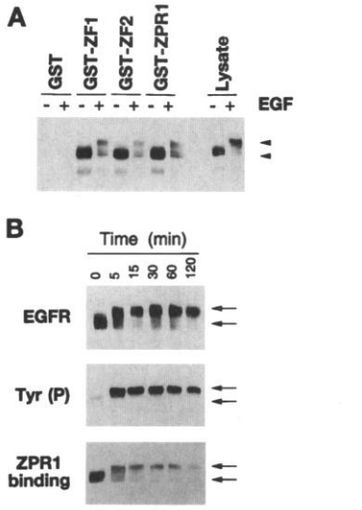

Fig. 3. Binding of the EGFR to ZPR1 is regulated by EGF. (**A**) A-431 cells were treated without and with 100 nM EGF for 5 min at 37°C (*10*). Soluble extracts were prepared and incubated with immobilized ZPR1 (GST-ZF1-A-ZF2) or ZPR1 zinc fingers (GST-ZF1 and GST-ZF2) (*19*). Bound EGFRs (arrowheads) were detected by protein immunoblot analysis (*18*). Control experiments were performed with immobilized GST. (**B**) A-431 cells were incubated for different periods of time with 100 nM EGF at 37°C (*10*). The level of EGFR expression, the extent of EGFR tyrosine phosphorylation [Tyr (P)], and the binding of EGFRs to immobilized ZPR1 (GST-ZPR1) was examined by protein immunoblot analysis (*18*) (all indicated by the arrowheads). (**C**) A-431 cells were treated without and with 100 nM EGF for 5 min at 37°C (*10*). Soluble extracts were prepared and immunoprecipitated with a rabbit polyclonal antibody to ZPR1 (*20*). Control experiments were performed with the use of preimmune serum. The ZPR1 immunoprecipitates were examined by protein immunoblot analysis with a monoclonal antibody to the EGFR (+ or −, respectively) (*18*). Arrowhead indicates the EGFR.

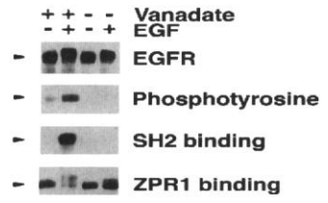

Fig. 4. ZPR1 binding to the EGFR is regulated by tyrosine phosphorylation. A-431 cells were incubated with 100 nM EGF for 5 min at 37°C (*10*). Soluble extracts were prepared in the presence and absence of the tyrosine phosphatase inhibitor orthovanadate. The amount of EGFR expression and tyrosine phosphorylation was examined by protein immunoblot analysis (*18*). The binding of EGFRs to the immobilized PLC-γ N-SH2 domain or to ZPR1 was examined by protein immunoblot analysis (*19*).

(Fig. 4). Control experiments designed to examine the role of Ser or Thr phosphorylation by investigating the requirement for Ser-Thr phosphatase inhibitors did not support a role for Ser or Thr phosphorylation in the regulation of EGFR binding to ZPR1 (*11*). These data indicate a primary role for tyrosine phosphorylation in the regulation of EGFR binding to ZPR1.

To test this hypothesis, we examined the interaction between ZPR1 and a mutated kinase-negative (K721R, where K is Lys and R is Arg) EGFR. The binding of ZPR1 to the kinase-negative EGFR was not altered by treatment of cells with EGF (*11*). Together, these data demonstrate that tyrosine phosphorylation is required for the regulation of EGFR binding to ZPR1.

The binding of ZPR1 to the nonactivated EGFR contrasts with the binding of the activated EGFR to proteins with SH2 or PTB domains (Fig. 4). To test whether the overexpression of ZPR1 would alter the interaction of the EGFR with SH2 or PTB proteins in vivo, we examined the effect of ZPR1 overexpression on the tyrosine phosphorylation of the SH2-PTB protein SHC (*14*). Protein immunoblot analysis of lysates prepared from the transfected cells demonstrated the presence of the EGFR and SHC polypeptides (Fig. 5A). Epitope-tagged ZPR1 was detected with the M2 monoclonal antibody (Fig. 5A). Treatment of the cells with EGF caused increased Ser, Thr, and Tyr phosphorylation and decreased electrophoretic mobility of the EGFR (*15*). Phosphotyrosine immunoblot analysis of EGFR immunoprecipitates (*11*) and SHC immunoprecipitates (Fig. 5B) demonstrated that EGF caused increased tyrosine phosphorylation of the EGFR and SHC polypeptides. The overexpression of ZPR1 caused a reduction in the EGF-stimulated tyrosine phosphorylation of both the EGFR (*11*) and SHC (Fig. 5B).

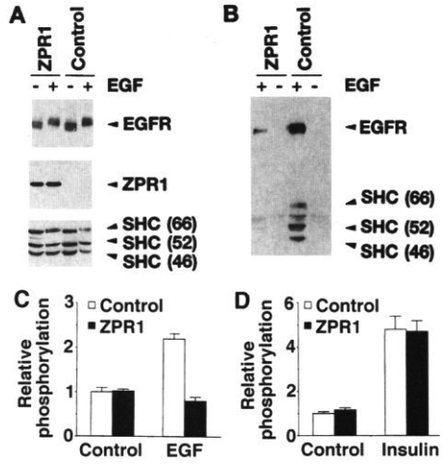

Fig. 5. ZPR1 overexpression inhibits EGF-stimulated SHC phosphorylation. COS cells were transfected with epitope-tagged ZPR1 (or were mock-transfected; control) and incubated without and with 100 nM EGF for 5 min at 37°C (*8, 10*). (**A**) The expression of EGFRs, epitope-tagged ZPR1, and SHC (66-kD, 52-kD, and 46-kD isoforms) was examined by protein immunoblot analysis of cell extracts prepared with lysis buffer (*10*). The EGFR and epitope-tagged ZPR1 were detected with the monoclonal antibodies 20.3.6 and M2, respectively (*18*). SHC was detected with a rabbit polyclonal antibody (*18*). (**B**) In an analysis similar to that in (A), SHC immunoprecipitates were examined by protein immunoblot analysis with the antibody to phosphotyrosine RC20 (*18*). (**C**) The effect of ZPR1 on EGFR tyrosine phosphorylation was examined with an in vitro protein kinase assay in the absence (control) or presence of 100 nM EGF (*21*). The phosphorylation of the EGFR was quantitated by PhosphorImager analysis. (**D**) The effect of ZPR1 on insulin receptor tyrosine phosphorylation was examined with an in vitro protein kinase assay in the absence (control) or presence of 100 nM insulin (*21*). The phosphorylation of the insulin receptor was quantitated by PhosphorImager analysis.

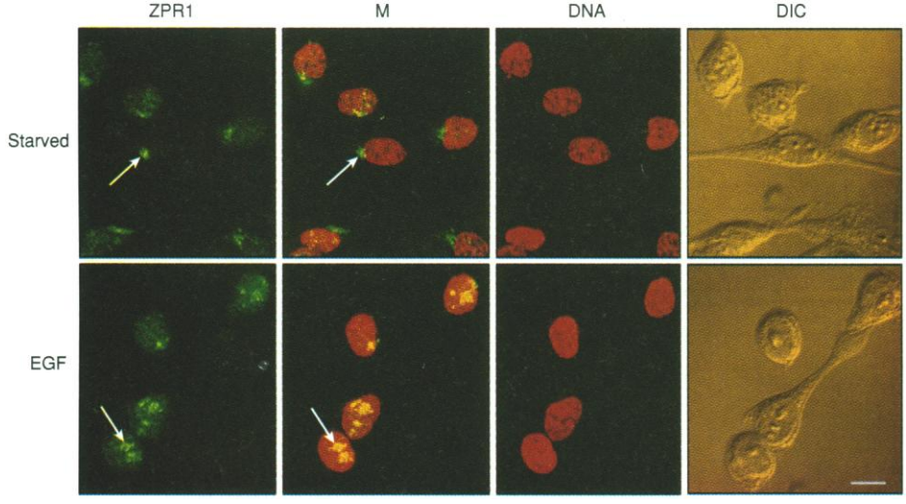

Fig. 6. Redistribution of ZPR1 from the cytoplasm to the nucleus in EGF-treated cells. A-431 cells were incubated in serum-free medium for 24 hours (starved) and treated with 100 nM EGF for 10 min at 37°C. The cells were fixed, permeabilized, and examined by double-label immunofluorescence laser scanning confocal microscopy (*22*). ZPR1 (fluorescein; green) and DNA (rhodamine; red) immunofluorescence are shown. Codistribution of ZPR1 and DNA immunofluorescence on the merged images (M) is presented (yellow). Arrows indicate reference points on the ZPR1 and merged images. A differential interference contrast image (DIC) is shown. The scale bar represents 10 μm.

Consistent with this reduced level of tyrosine phosphorylation, ZPR1 overexpression decreased the EGF-stimulated formation of SHC-EGFR complexes that were detected by immunoblot analysis of SHC immunoprecipitates with antibodies to the EGFR (*11*) and phosphotyrosine (Fig. 5B). These data indicate that ZPR1 overexpression causes inhibition of EGF-stimulated tyrosine phosphorylation in vivo. To examine the specificity of the inhibition of tyrosine phosphorylation caused by ZPR1, we investigated the effect of ZPR1 on the tyrosine phosphorylation of the EGF and insulin receptors. In vitro protein kinase assays demonstrated that ZPR1 inhibited the tyrosine phosphorylation of the EGFR (Fig. 5C), but not of the insulin receptor (Fig. 5D). Together, these data demonstrate that ZPR1 overexpression causes a partial inhibition of EGF-stimulated tyrosine kinase activity. It is possible that the interaction of ZPR1 with the nonactivated EGFR (Fig. 3) may contribute to the inhibition of EGF-stimulated tyrosine phosphorylation caused by overexpressed ZPR1.

The subcellular location of ZPR1 in serum-starved and EGF-treated cells was examined by immunofluorescence analysis (Fig. 6). The ZPR1 protein was widely distributed in the cytoplasm of serum-starved cells (Fig. 6). In addition, an accumulation of ZPR1 was detected in the perinuclear region of the cells (Fig. 6). This perinuclear region co-localized with a Golgi-associated antigen (*16*). EGFRs were also detected in this perinuclear region and at the cell periphery (*16*). To test whether the cytoplasmic ZPR1 protein co-localized with the EGFR, we performed double-label immunofluorescence analysis with antibodies to ZPR1 and the EGFR. Partial co-localization of ZPR1 with a subpopulation of EGFRs was observed (*16*). These data demonstrate a cytoplasmic localization of both ZPR1 and the EGFR.

Treatment of the cells with EGF altered the subcellular distribution of the EGFRs (*16*). The punctate staining of EGFRs observed after EGF treatment is likely to reflect the internalization and sequestration of the EGFRs in an endosomal compart-

ment. EGF was also found to cause the partial redistribution of ZPR1 within the cell. Double-label immunofluorescence analysis of ZPR1 and a nuclear marker (DNA) in EGF-treated cells demonstrated that the ZPR1 protein was detected in the nucleus (Fig. 6). Differential interference contrast microscopy confirmed that ZPR1 was located in the nuclei of EGF-treated cells (Fig. 6). Double-label immunofluorescence studies demonstrated that the nuclear ZPR1 co-localized with fibrillarin and RNA polymerase I but did not co-localize with the splicing factor SC35 or p80 coilin (*16*). Together, these data demonstrate that the cytoplasmic ZPR1 protein accumulates in the nuclei of activated cells.

ZPR1 may function in multiple physiological processes. We demonstrated here that ZPR1 interacts with a group of tyrosine kinase receptors, including the EGF and PDGF receptors. The ZPR1 protein may also interact with nucleic acids, proteins, or other biomolecules. The binding of ZPR1 to the nonactivated EGFR indicates that ZPR1 may contribute to the function of the basal EGFR complex. In addition, ZPR1 represents a class of signaling molecules that are released from the receptor after activation. Nuclear accumulation of ZPR1 in activated cells suggests that this protein may participate in signal transduction to the nucleus. It is also possible that ZPR1 may function in processes that are unrelated to receptor tyrosine kinase signal transduction.

REFERENCES AND NOTES

1. A. Ullrich and J. Schlessinger, *Cell* **61**, 203 (1990); J. Schlessinger and A. Ullrich, *Neuron* **9**, 383 (1992).
2. C. A. Koch, D. Anderson, M. F. Moran, C. Ellis, T. Pawson, *Science* **252**, 668 (1991); T. Pawson and G. D. Gish, *Cell* **71**, 359 (1992); W. M. Kavanaugh and L. T. Williams, *Science* **266**, 1862 (1994); W. M. Kavanaugh, C. W. Turck, L. T. Williams, *Ibid.* **268**, 1177 (1995); P. Bork and B. Margolis, *Cell* **80**, 693 (1995).
3. L. M. Roy, C. K. Gittinger, G. F. Landreth, *J. Cell. Physiol.* **146**, 63 (1991); J. C. den Hartigh, P. M. van Bergen en Henegouwen, A. J. Verkleij, J. Boonstra, *J. Cell Biol.* **119**, 349 (1992); A. M. Gronowski and P. J. Bertics, *Endocrinology* **133**, 2836 (1993); *ibid.* **135**, 2198 (1995).
4. R. Y. Wu and G. N. Gill, *J. Biol. Chem.* **269**, 25085 (1994).
5. M. Rothe, S. C. Wong, W. J. Henzl, D. V. Goeddel, *Cell* **78**, 681 (1994); H. M. Hu, K. O'Rourke, M. S. Boguski, V. M. Dixit, *J. Biol. Chem.* **269**, 30069 (1994); G. Cheng *et al.*, *Science* **267**, 1494 (1995); G. Mosialos *et al.*, *Cell* **80**, 389 (1995).
6. A ZPR1 cDNA fragment was isolated from a two-hybrid screen [S. Fields and O. K. Song, *Nature* **340**, 245 (1989)] of a mouse embryo cDNA library with the use of the yeast strain L40 [MAT**a** *his*Δ*200 trp1-901 leu2-3,112 ade2 LYS::(lexAop)$_4$-HIS URA3::(lexAop)$_8$-lacZ*] [A. B. Vojtek, S. M. Hollenberg, J. A. Cooper, *Cell* **74**, 205 (1993)]. The bait plasmid expressed the LexA DNA binding domain fused to the COOH-terminal region of the human EGFR (residues 908 to 1186). Twenty million yeast transformants were examined for growth on media in the absence of histidine. Positive clones were confirmed by measurement of LacZ expression. Sequence analysis identified six independent ZPR1 cDNA clones that were fused in-frame to the activation domain of VP16. We obtained a full-length ZPR1 clone by screening a mouse NIH 3T3 cell cDNA library (Stratagene) with a random-primed ZPR1 cDNA fragment. The ZPR1 cDNA (2162 bp) was sequenced with an Applied Biosystems model 373A machine. ZPR1 expression in murine tissues was examined by Northern blot analysis of polyadenylated mRNA isolated from various murine tissues (Clontech) with a ZPR1 cDNA probe labeled with [α-^{32}P]cytidine triphosphate by random priming (Amersham International PLC).
7. We dialyzed against water 6 mg of purified glutathione S-transferase (GST)–Zpr1 and lyophilized it. The protein was solubilized by incubation for 30 min at 65°C in concentrated nitric acid (0.5 ml). The amount of zinc was determined by inductively coupled plasma emission spectroscopy.
8. The Flag epitope (-Asp-Tyr-Lys-Asp-Asp-Asp-Asp-Lys-; Immunex) was inserted between codons 1 and 2 of the ZPR1 cDNA by insertional overlapping polymerase chain reaction (PCR) [S. N. Ho, H. D. Hunt, R. M. Horton, J. K. Pullen, L. R. Pease, *Gene* **77**, 51 (1989)]. A similar PCR procedure was used to replace Cys^{80}, Cys^{83}, Cys^{288}, and Cys^{291} with Ser. We constructed ZPR1 expression vectors by subcloning the ZPR1 cDNA in the Hind III and Eco RI sites of pCDNA3 (Invitrogen). Bacterial ZPR1 expression vectors were constructed by subcloning PCR fragments of the ZPR1 cDNA in the Eco RI and Xho I sites of pGEX-5X (Pharmacia LKB Biotechnology). The wild-type human EGFR and a mutant receptor truncated at residue 958 have been described [R. J. Davis, *J. Biol. Chem.* **263**, 9462 (1988); A. J. Ekstrand, N. Sugawa, C. D. James, V. P. Collins, *Proc. Natl. Acad. Sci. U.S.A.* **89**, 4309 (1992)]. The EGFR mutant truncated at residue 908 was prepared by restriction digestion with Bgl II. The sequences of all plasmids were confirmed by automated sequencing with an Applied Biosystems model 373A machine.
9. A smaller amount of binding was observed in experiments with ZPR1 proteins containing the B domain. This may be caused by a function of the B domain to negatively regulate EGFR binding. Alternatively, the presence of the B domain may induce partially improper folding of bacterially expressed ZPR1 protein.
10. A-431 and COS-1 cells were obtained from the American Type Culture Collection and were maintained in Dulbecco's modified Eagle's medium supplemented with calf serum (5%) (Gibco-BRL). Chinese hamster ovary (CHO) cells expressing the human wild-type [Lys^{721}]EGFR and the mutated, kinase-negative [Arg^{721}]EGFR have been described [J. L. Countaway, A. C. Nairn, R. J. Davis, *J. Biol. Chem.* **267**, 1129 (1992)]. These cells were maintained in Ham's F-12 medium supplemented with 5% fetal bovine serum (Gibco-BRL). Transfection studies were performed with the lipofectamine reagent (Gibco-BRL) and purified plasmid DNA (*8*). The cells were cultured in 100-mm dishes and solubilized with 1 ml of lysis buffer [20 mM tris (pH 7.4), 2 mM EDTA, 2 mM sodium pyrophosphate, 25 mM sodium β-glycerophosphate, 1 mM sodium orthovanadate, 25 mM NaCl, 0.1% Triton X-100, 10% glycerol, 1 mM phenylmethylsulfonyl fluoride (PMSF), 10 μg/ml of leupeptin, and 10 μg/ml of aprotinin]. Some extracts were prepared with the use of lysis buffer without the Ser-Thr phosphatase inhibitors β-glycerophosphate and pyrophosphate or the Tyr phosphatase inhibitor orthovanadate. We performed calpain cleavage of the EGFRs by harvesting cells in lysis buffer without EDTA, PMSF, leupeptin, and aprotinin. The extracts were clarified by centrifugation at 100,000*g* for 20 min at 4°C.
11. Z. Galcheva-Gargova, unpublished data.
12. M. Gregoriou, A. C. Willis, M. A. Pearson, C. Crawford, *Eur. J. Biochem.* **223**, 455 (1994).
13. S. R. Hubbard, L. Wei, L. Ellis, W. A. Hendrickson, *Nature* **372**, 746 (1994).
14. G. Pelicci *et al.*, *Cell* **70**, 93 (1992).
15. EGF causes increased phosphorylation and reduced electrophoretic mobility of the EGFR during SDS–polyacrylamide gel electrophoresis (SDS-PAGE). Contributions to the gel shift arise from increased Ser, Thr, and Tyr phosphorylation. The EGFR gel shift was observed in EGF-treated cells overexpressing ZPR1 (Fig. 5A). As ZPR1 inhibits EGFR tyrosine phosphorylation (Fig. 5B), the gel shift observed indicates that ZPR1 does not inhibit the EGF-stimulated Ser and Thr phosphorylation of the EGFR. This increased Ser and Thr phosphorylation is caused, in part, by activation of cytoplasmic protein kinases [J. L. Countaway, I. C. Northwood, R. J. Davis, *J. Biol. Chem.* **264**, 10828 (1989)]. Thus, the reduced EGF-stimulated tyrosine phosphorylation observed in cells overexpressing ZPR1 (Fig. 5B) is not sufficient to completely block signaling by the EGFR. Indeed, control experiments demonstrated that EGF can activate the MAP kinase ERK2 in cells overexpressing ZPR1.
16. K. N. Konstantinov and Z. Galcheva-Gargova, unpublished data.
17. Single-letter abbreviations for the amino acid residues are as follows: A, Ala; C, Cys; D, Asp; E, Glu; F, Phe; G, Gly; H, His; I, Ile; K, Lys; L, Leu; M, Met; N, Asn; P, Pro; Q, Gln; R, Arg; S, Ser; T, Thr; V, Val; W, Trp; and Y, Tyr.
18. Proteins were fractionated by SDS-PAGE and transferred to a polyvinylidene difluoride membrane (Immobilon-P; Millipore). The blots were probed with the monoclonal antibody to phosphotyrosine PY20 (ICN Biomedicals), the anti-phosphotyrosine horseradish peroxidase conjugate RC20 (Transduction Labs), a monoclonal antibody to HA (BabCo), the monoclonal antibody to Flag M2 (IBI-Kodak), the monoclonal antibody to the EGFR 20.3.6, a rabbit polyclonal antibody to the PDGF receptor β (Upstate Biotechnology), the monoclonal antibody to the IGF-1 receptor αIR3 (Oncogene Science), the monoclonal antibody to the insulin receptor CT-1, the rabbit polyclonal antibody to TrkA 203, a rabbit polyclonal antibody to SHC (Transduction Labs), and a rabbit polyclonal antibody to ZPR1 that was prepared with the synthetic peptide NDMKTEGYEAGLAPQ (*17*) as an antigen (Research Genetics). Immune complexes were detected by enhanced chemiluminescence (Amersham).
19. GST, GST-ZPR1, and GST-PLC-γ-N-SH2 were expressed in bacteria and purified by glutathione-agarose affinity chromatography [S. B. Smith and K. S. Johnson, *Gene* **67**, 31 (1988)]. The GST fusion proteins (5 μg) were immobilized on glutathione-agarose. The binding of EGFRs was assayed by two procedures. In vitro–translated, [^{35}S]methionine-labeled EGFRs were incubated in lysis buffer with immobilized GST fusion proteins at 4°C for 1 hour. The agarose beads were washed extensively with lysis buffer, and bound EGFRs were detected by SDS-PAGE and PhosphorImager analysis (Molecular Dynamics). Binding assays were also performed by incubation of the immobilized GST fusion proteins (5 μg) with a soluble cell extract (1 ml) prepared from 2.5×10^5 cells in lysis buffer (*10*). The binding reaction was incubated at 22°C for 1 hour. The agarose beads were washed extensively with lysis buffer, and bound EGFRs were detected by protein immunoblot analysis. The binding of TrkA was examined with the use of extracts of Sf9 cells infected with a TrkA baculovirus. The binding of the insulin receptor, IGF-1 receptor, PDGF receptor β, MAP kinases, and MAP kinase kinases was examined with extracts prepared from transfected COS cells. The expression vectors were pCMV5-PDGF-Rβ, pCMV5-INS-R, pCMV5-IGF1-R, pCMV-Flag-p38 [J. Raingeaud *et al.*, *J. Biol. Chem.* **270**, 7420 (1995)], pCDNA3-Flag-JNK1 [B. Dérijard *et al.*, *Cell* **76**, 1025 (1994)], pCMV-HA-ERK2, pCMV-HA-MKK1, and pRSV-Flag-MKK3 and pCDNA3-Flag-MKK4 [B. Dérijard *et al.*, *Science* **267**, 682 (1995)].
20. A-431 cells cultured in 100-mm dishes were serum-starved (12 hours) and treated without and with 100 nM EGF for 5 min at 37°C (*10*). Soluble extracts were prepared with 1 ml of lysis buffer (*10*). ZPR1 was immunoprecipitated with a rabbit polyclonal antibody that was prepared with the antigen GST-ZPR1 (residues 292 to 416). Control experiments were done with preimmune serum. The immunoprecipitates were washed three times with 20 mM tris (pH 7.4), 2 mM EDTA, 137 mM NaCl, 2 mM sodium pyrophosphate, 25 mM sodium β-glycerophosphate, 1 mM sodium orthovanadate, 1% Triton

X-100, 0.5% deoxycholate, 0.1% SDS, 10% glycerol, 1 mM PMSF, 10 μg/ml of leupeptin, and 10 μg/ml of aprotinin. The ZPR1 immunoprecipitates were examined by protein immunoblot analysis with the monoclonal EGFR antibody 20.3.6 (*18*).

21. Membranes were prepared from A-431 cells and from CHO T cells that express the human insulin receptor. Briefly, the cells were serum-starved for 2 hours and washed with Hepes-buffered saline supplemented with 10 mM EDTA. The cells were lysed in 20 mM tris (pH 7.4), 2 mM EDTA, 2 mM sodium pyrophosphate, 25 mM sodium β-glycerophosphate, 1 mM sodium orthovanadate, 25 mM NaCl, 1 mM PMSF, 10 μg/ml of leupeptin, and 10 μg/ml of aprotinin. Nuclei and unbroken cells were removed by centrifugation, and membranes in the supernatant fraction were recovered by centrifugation (30 min) at 100,000*g*. The membranes were washed with 25 mM Hepes (pH 7.4). Protein kinase assays were performed with 100 μg of membranes incubated with 5 μM [γ-^{32}P]adenosine triphosphate (10 μCi/nmol), 50 mM Hepes, 12 mM $MgCl_2$, 2.5 mM $MnCl_2$, and 100 μM sodium orthovanadate (final volume = 40 μl) at 4°C. The effect of adding 5 μg of GST or GST-ZPR1 was examined. The EGFR phosphorylation was examined in assays without and with 100 nM EGF, and the reactions were terminated after 30 s. The insulin receptor phosphorylation was examined in assays without and with 100 nM insulin, and the reactions were terminated after 2 min. The incorporation of [^{32}P]phosphate into the receptors was determined after immunoprecipitation by SDS-PAGE and PhosphorImager analysis.
22. A-431 cells were cultured on glass cover slips (22-mm squares; Corning). The cells were rinsed briefly with phosphate-buffered saline (PBS) and fixed at −20°C with methanol (5 min) and acetone (2 min). DNA was detected with the monoclonal antibody 1.D12 [B. L. Kotzin *et al.*, *J. Immunol.* **133**, 2554 (1984)], EGFRs were detected with the monoclonal antibody 528 [T. Kawamoto *et al.*, *Proc. Natl. Acad. Sci. U.S.A.* **80**, 1337 (1983)] (American Type Culture Collection), the Golgi region was detected with a human antibody to a Golgi-associated antigen [M. J. Fritzler, K. J. Griffith, E. K. L. Chan, *Mol. Biol. Cell* **5**, 1043 (1994)], and ZPR1 was detected with a rabbit polyclonal antibody to the peptide NDMK-TEGYEAGLAPQ (*17, 18*). The incubation with the primary antibodies (1 hour) was done at 25°C. The cover slips were washed three times with PBS and incubated (1 hour) with species-specific secondary antibodies coupled to fluorescein or rhodamine (Caltag Laboratories). The cover slips were washed three times with PBS and mounted on slides with Vectashield media (Vector Laboratories). Control experiments with preimmune immunoglobulin and competition analysis with antigen demonstrated the specificity of the ZPR1 immunofluorescence. Microscopy was done with an MRC-600 confocal laser scanning microscope with an argon-krypton mixed gas laser (Bio-Rad) fitted to a Zeiss Axiovert epifluorescence microscope with an oil immersion objective lens (1.4 numerical aperture; 63×). Images were collected from a single focal plane (approximately 0.4 μm) with the use of Kalman averaging of 30 scans (Bio-Rad COMOS program). The rhodamine and fluorescein images were collected simultaneously, digitized, and subsequently merged. Differential interference contrast (DIC) images were collected after fluorescence imaging. The images were recorded on Kodak Ektar 25 film.
23. We thank the following for reagents: A. Ross for the TrkA baculovirus, A. Kazlauskis for pCMV5-PDGF-Rβ, R. L. Lewis for pCMV5-INS-R, and pCMV5-IGF1-R, M. Weber for pCMV-HA-ERK2, N. Ahn for pCMV-HA-MKK1, M. Hayman for the monoclonal antibody to the EGFR 20.3.6, K. M. Pollard for the fibrillarian antibody 72B9, K. Siddle for the monoclonal antibody to the insulin receptor CT-1, A. Ross for the rabbit polyclonal antibody to TrkA 203, R. L. Rubin for monoclonal antibody 1.D12, and E. K. L. Chan for human antibody to a Golgi-associated antigen. We also thank W. Royer for assistance with computer graphics; T. Gilbert for assistance with spectroscopic analysis; and M. Roberts for secretarial assistance. Confocal microscopy was supported by the Lucille P. Markey Charitable Trust. R.J.D. is an Investigator of the Howard Hughes Medical Institute. Supported by grant R01-CA58396 from the National Cancer Institute.

4 December 1995; accepted 18 April 1996

Punctuated Evolution Caused by Selection of Rare Beneficial Mutations

Santiago F. Elena,* Vaughn S. Cooper, Richard E. Lenski

For more than two decades there has been intense debate over the hypothesis that most morphological evolution occurs during relatively brief episodes of rapid change that punctuate much longer periods of stasis. A clear and unambiguous case of punctuated evolution is presented for cell size in a population of *Escherichia coli* evolving for 3000 generations in a constant environment. The punctuation is caused by natural selection as rare, beneficial mutations sweep successively through the population. This experiment shows that the most elementary processes in population genetics can give rise to punctuated evolutionary dynamics.

The debate over punctuated equilibria (*1*) in evolutionary biology revolves around two distinct issues. One issue is whether, and how often, the actual dynamics of evolutionary change are punctuated by alternating periods of rapid change and relative stasis. This is an empirical issue, and the answer may depend on the coarseness of the time scale over which observations are made (*2*). The other issue concerns the processes responsible for any punctuation that does occur. It has been argued that punctuation involves the complex population genetic processes that are believed to play an important role in speciation (*3*). For example, punctuation might be precipitated by population bottlenecks that promote random genetic drift and rapid transitions between alternative adaptive peaks (*4*). This view may be supported by an association between rates of anagenesis (change within a lineage) and cladogenesis (branching of lineages), but the generality and causal mechanism of this association have been disputed (*1*, *3*, *5*).

Our study builds upon earlier work (*6*, *7*) on evolution in experimental populations of the bacterium *E. coli* B. Each population was founded from a single cell, allowed to expand to $\sim 5 \times 10^8$ cells, and then serially transferred for 1500 days (10,000 generations) in glucose-limited minimal medium (*8*). At each transfer, the minimum population size was $\sim 5 \times 10^6$ cells. The strain used in this experiment lacks any mechanism for genetic exchange; mutations therefore provided the sole source of genetic variation. Some 10^6 mutations occurred every day in each population (*9*). We did not artificially select cells on the basis of any phenotypic property. However, any mutation that conferred some competitive advantage in exploiting the experimental environment would have been favored by natural selection. Such an advantage might involve more rapid uptake of glucose, more efficient catabolism, or any number of other physiological changes (*10*). We monitored two characters, mean fitness and average cell size, in the evolving populations. Fitness was measured by allowing derived and ancestral cells to compete against one another, and it is expressed as the ratio of their realized growth rates (*6*).

When the evolving populations were sampled at a frequency of once every 500 generations, the trajectories for both mean fitness and average cell size were well fit by a hyperbolic model (*7*); that is, the rate of change for each character decreased over time from an initially rapid rate, such that the character appeared to be approaching some asymptotic value. However, when mean fitness was measured every 100 generations over the period of fastest change (the first 2000 generations), a step-function model, in which periods of stasis were interrupted by episodes of rapid change, gave a better fit to the data than did the hyperbolic model (*7*). Evidently, it was necessary to make measurements at sufficiently high frequency to resolve the punctuated dynamics.

Steplike dynamics are predicted for mean fitness by a simple model in which successive beneficial mutations sweep through an evolving population by natural selection (*5*, *6*, *11*). Consider the initial appearance of a beneficial mutation (which

Center for Microbial Ecology, Michigan State University, East Lansing, MI 48824, USA.

*To whom correspondence should be addressed. E-mail: selena@ant.css.msu.edu